Heterogenized molecular (pre)catalysts for water oxidation and oxygen reduction

Ham, C.J.M. van der

4 | *In situ* generated copper-phenanthroline complexes as catalysts for the oxygen reduction reaction

Abstract

The oxygen reduction reaction was investigated with an *in situ* generated copper phenanthroline complex using different ratios of ligand to copper. A structural investigation of the *in situ* generated complex by EPR spectroscopy showed the formation of complexes in two different geometries. The 1:1 complex has an elongated octahedron geometry and is an active oxygen reduction catalyst. In case of this species, reduction of Cu^{II} is not reversible. At a higher 1,10-phenanthroline to copper ratio a complex is generated with a trigonal bipyrimidal geometry. In this case the complex has a well-defined redox couple, but is not active towards the oxygen reduction reaction. There is thus a paradox wherein a decision has to be made between catalytic activity and stability of the complex. Under reductive conditions the possibility of forming a metallic copper layer on the electrode surface is ever present. A strategy to prevent the active 1:1 complex form forming an electrocatalytically active copper layer is proposed. This strategy is discussed in detail in Chapter 5.

"Tell me, tutor,' I said. 'Is revenge a science, or an art?"

Mark Lawrence in *Prince of Thorns*

In preparation for publication

4.1 Introduction

The oxygen reduction reaction is of interest for the development of efficient fuel cells wherein it is the counter reaction to the hydrogen oxidation reaction. In order to find an excellent catalyst for the oxygen reduction reaction, the binding energy of all intermediates of the catalytic cycle wherein oxygen reduction takes place need to be optimized simultaneously. This will result in a potential energy landscape wherein all redox intermediates within the catalytic cycle are found at the equilibrium potential of water. Under these conditions catalysis should start at the equilibrium potential. Since the various catalytic intermediates bind in a very similar manner to a heterogeneous surface, it is not possible to align these to the same potential energy. This inability to align the catalytic intermediates from an energetic point of view is referred to as the scaling relationships, first described by Nørskov.[1] Due to such scaling relations the oxygen reduction reaction has a theoretical minimum overpotential of 0.41 V at a metal surface.[2]

In nature, laccase is an efficient copper-based enzyme for the reduction of oxygen to water.[3] Due to the complex protein backbone the reaction pathway for the oxygen reduction reaction is different to that of heterogeneous catalysts. This difference in reaction mechanism leads to a different potential energy landscape and a lowering of the overpotential of the oxygen reduction reaction compared to heterogeneous surfaces is observed.

The difficulty of using copper as a molecular oxygen reduction catalyst lies in the fast ligand exchange kinetics of copper. The exchange rate of water ligands at a Cu^{II} center is in the range of 10^8 ligands per second.[4, 5] The low barrier for ligand exchange on copper complexes causes other ligands to be replaced at a high exchange rate as well. By decoordinating the ligands from the metal center under reductive conditions a metallic copper layer can be formed on the surface of the electrode (see for example Chapter 3). Using 3,5-diamino-1,2,4-triazole (DAT) as a ligand, a dinuclear $Cu_2(DAT)_2$ complex is formed,[6] which was claimed to be a very active oxygen reduction catalyst.[7] The structure of the formed catalyst is highly dependent on the reaction conditions.[8] The complex $[Cu_2(DAT)_2(\mu\text{-}OH_2)(H_2O)_4(SO_4)](SO_4) \cdot 3.5H_2O$ synthesised *ex situ* forms a deposit on the electrode surface during oxygen reduction.[9] Moreover, when the complex is dropcasted onto a glassy carbon electrode, the loss of DAT from the complex is observed and a Cu(0) deposit is formed on the surface of the electrode. This surface deposit is the active

oxygen reduction catalyst.[9] Therefore, one needs to be careful to the nature of the active catalyst in copper-mediated oxygen reduction. Under very low concentrations of DAT, a copper layer is formed on a glassy carbon electrode, which is a good catalyst for carbon dioxide reduction.[8]

Anson and coworkers reported oxygen reduction using physisorbed copper complexes with 1,10-phenanthroline based ligands.[10–12] The first report describes a copper complex with a 4,7-diphenyl-1,10-phenanthrolinedisulfonate (DPP) ligand which is forming a $[Cu\text{-}(DPP)_2H_2O]^{2-}$ complex in water.[11] The complex has a very large interaction with a pyrolytic graphite electrode, causing the complex to adsorb on the working electrode spontaneously. Using the charge transfer of the redox couple, the surface coverage of the complex was determined to be 8.5×10^{-10} mol cm^{-2}, indicating multiple layers of complex on the electrode surface. Two different species are observed in the cyclic voltammetry, of which the first is claimed to be a Cu^{II} complex with two ligands and water ligated to the copper center. The copper sits in a tetragonal geometry, with one of the axial position being unavailable due to surface adsorption. The second structure is claimed to be a tetrahedral Cu^{I} complex with only two DPP ligands coordinated. This indicates a substantial structural change upon reduction from Cu^{II} to Cu^{I} and might forestall the adsorption of the complex on the electrode surface. The cyclic voltammetry did not change when an excess of DPP was added to the electrolyte solution, which is an indication that under these conditions no complex is present with only one DPP ligand. During oxygen and H_2O_2 reduction, the $[Cu^{II}(DPP)_2H_2O]^{2-}$ complex is suggested to be reduced to $[Cu^{I}(DPP)_2H_2O]^{3-}$, which is the active species that binds dioxygen. Deactivation of the catalyst was suggested to occur through formation of $[Cu^{I}(DPP)_2]^{3-}$ via dissociation of an aqua ligand from the active oxygen reduction catalyst $[Cu^{I}(DPP)_2H_2O]^{3-}$. It can be reactivated by oxidizing the complex to the $[Cu^{II}(DPP)_2]^{2-}$ complex, which will spontaneously form the stable $[Cu^{II}(DPP)_2H_2O]^{2-}$, restoring the initial catalytic activity.

Using different phenanthroline derivatives, Zhang and Anson found that the 4,7-dimethyl-1,10-phenanthroline (DMP) ligand performs best in the copper mediated oxygen reduction.[10] This was correlated to a shift of the Cu^{I}/Cu^{II} couple to higher potentials compared to copper complexes with 1,10-phenanthroline, 2-2'-bipyridine, 6,6-dimethyl-2,2'-bipyridine and 6-methyl-2,2'-bipyridine ligands. Similar to the complex $[Cu^{II}(DPP)_2H_2O]^{2+}_{ads}$ *vide supra*, the complex $[Cu^{II}(DMP)]^{2+}$ adsorbs onto the graphite working electrode spontaneously, as is observed

from the shape of the redox couples in the cyclic voltammogram. The formation of both complexes $[Cu^{II}(DMP)]^{2+}_{ads}$, with only one ligand coordinated, and $[Cu^{II}(DMP)_2]^{2+}_{ads}$ are observed electrochemically. The adsorbed complex with one ligand is predominantly observed when $CuSO_4$ is present in solution, whereas in presence of DMP in the electrolyte solution, the $[Cu^{II}(DMP)_2]^{2+}_{ads}$ complex is observed. This indicates the complex can reversibly form the complex with one and with two DMP ligands, depending on the presence of Cu^{2+} or DMP in the electrolyte solution. Oxygen and H_2O_2 reduction is observed in presence of the $[Cu^{II}(DMP)]^{2+}_{ads}$ complex, with an onset potential of 0.79 V *versus* RHE at pH 5. This is in contrast to the DPP case, where the active species was proposed to have two bidentate ligands coordinated. Due to the adsorption of the active species to pyrolytic graphite and the absence of any spectroscopic data of Cu at such materials, prompted us to investigate the ORR at copper phenanthroline species under better defined reaction conditions.

Here we report oxygen reduction by *in situ* generated copper-phenanthroline complexes. Since the ligands have a very strong interaction with pyrolytic graphite electrodes and the difficulty to characterize, gold electrodes were selected as the working electrode. The structure of the *in situ* generated complexes was investigated using EPR spectroscopy. Other ligands were investigated as well, DMP is an interesting ligand for a copper complex as it gives higher activity than copper-phenanthroline when adsorbed on graphite electrodes.[10] Bipy is interesting as ligand as it is very similar in structure as 1,10-phenanthroline, but allows for rotation between the phenyl rings, giving the complex more flexibility.

4.2 Experimental

4.2.1 Materials

1,10-phenanthroline (Sigma Aldrich, 97%), 2-2'-bipyridine (Alfa Aesar, 99%), 4,7-dimethyl-1,10-phenanthroline (Sigma Aldrich) and $Cu(OTf)_2$ (Alfa Aesar, $\geq$ 99%) were used as received.

Electrolyte solutions were prepared with $HClO_4$ (Merck suprapur, 70 %), HCl (Merck, 37 %), Na_2HPO_4 (Merck, 99.9%), NaH_2PO_4 (Merck, 99.9 %), NaCl (Merck, 99.9 %) and were prepared with MilliQ water ($>$ 18.2 MΩ cm resistivity).

Argon and dioxygen (5.0) were purchased from Linde Gas.

4.2.2 Electrochemical methods

All electrochemical experiments were performed on an Autolab PGSTAT 128N with integrated EQCM module in one-compartment 25 ml glass cells in three-electrode setups. A gold working electrode (99.995 %, Alfa Aesar, 0.05 cm^2 geometric surface area) was used in a hanging meniscus configuration. Platinum (99.99%, Alfa Aesar) was used as a counter electrode and a Ag/AgCl (3 M KCl) purchased from Autolab was used as reference electrode. The potentials were adjusted to the reversible hydrogen electrode (RHE) scale by addition of 0.446 V to the potential *versus* Ag/AgCl.

The Au electrode was cleaned by oxidation at 10 V *versus* a graphite rod counter electrode in 10% H_2SO_4 for 30 s. This was followed by a 6 M HCl bath for 20 s, followed by flame annealing. The electrode was then electrochemically polished by cycling between 0 and 1.75 V *versus* RHE (E_{start} = 0.7 V) at 1 V s^{-1} in 0.1 M $HClO_4$.

Prior to experiments, the electrolyte solution was deaerated for at least 20 minutes using argon. Oxygen reduction experiments were performed in 0.05 M NaH_2PO_4, 0.05 M Na_2HPO_4, 0.05 M NaCl and 0.6 mM HCl. In case of catalytic experiments, 0.1 mM $Cu(OTf)_2$ was added to the electrolyte solution while a 1 mM 1,10-phenanthroline concentration was used, unless denoted differently. Prior to oxygen reduction experiments, oxygen was bubbled through the electrolyte for at least 20 minutes, while during experiment, oxygen was blown over the solution.

4.2.3 EPR spectroscopy

The EPR experiments were performed on a Bruker EMXplus X-band. Simulation of the spectra was performed using the W95EPR software. The spectra were simulated using the W95EPR software. The EPR samples were prepared by dissolving different concentrations, ranging from 1 mM to 0.1 mM, of 1,10-phenanthroline together with 0.1 mM Cu^{II}, 0.1 M phosphate buffer, 0.05 M NaCl acidified to pH 4 using HCl. The samples were recorded at 77 K.

4.3 Results

4.3.1 EPS spectroscopy of an *in situ* generated copper-phenanthroline complex

Cu^{2+} is insoluble in in a perchlorate solution in absence of any ligand. To avoid precipitation of copper from the reaction mixture, an electrolyte based on chloride was selected, which kept all copper species in solution prior to the electrochemistry experiments. Due to the fast ligand exchange kinetics of copper, bidentate ligands were expected to readily decoordinate immediately leading to small concentrations of free Cu^{2+}. To counter formation of substantial concentration of free copper in solution, a high ratio of 1,10-phenanthroline *versus* the copper in solution will ensure that most of the complex in solution will have two 1,10-phenanthroline ligands in the solution at all times. This should lead to a well-defined molecular complex, but does not ensure a catalytically active species. In this chapter, the structure of the ligands in solution was investigated with EPR spectroscopy, followed by an investigation of the redox behavior of the *in situ* generated complexes. Finally, the electrocatalytic behavior of the complexes is investigated for the oxygen reduction reaction.

EPR spectroscopy is powerful tool in the characterization of compounds which have at least one unpaired electron. As Cu^{II} has 9 d-electrons, one electron will always be unpaired. Cu^{II} complexes generally adopt two types of geometries: the trigonal bipyramidal and elongated octahedron geometry. Depending on the geometry of the complex, the singly occupied molecular orbital (SOMO) of the complex is either the d_{z^2} or the $d_{x^2-y^2}$ orbital. For the trigonal bipyrimidal geometry the SOMO is the d_{z^2} orbital, whereas a Cu^{II} complex in the elongated octahedron geometry has the $d_{x^2-y^2}$ as SOMO. The value of the empirical parameter g, comparable to the chemical shift in NMR spectroscopy, is determined in the x-, y- and z-direction.[13] The relative positions of the g-values can be determined by Equation 4.1, where *i* = *x*,*y* or *z*, *n* is the degree of orbital mixing, λ is the spin-orbit coupling constant, E_0 and E_n are the energies of the ground and the exited states.

$$g_i = g_e \pm \frac{n\lambda}{E_0 - E_n} \tag{4.1}$$

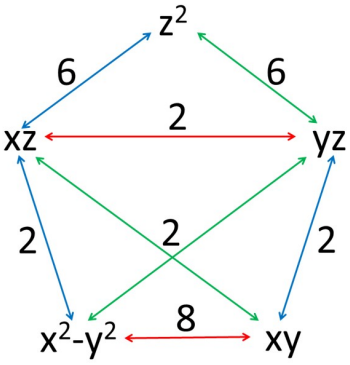

Figure 4.1: The magic pentagon for the determination of shift of g-values in EPR spectroscopy. The colors represent the direction of the overlap: green is in the x-direction, blue is in the y-direction and red is in the z-direction.

The direction of the shift, represented by $\pm$ depends whether the orbital that mix with the SOMO are filled (+) or empty (-). For Cu^{II} complexes, all orbitals except the SOMO are filled and the g-values increase as a result of orbital mixing. The shift of the g-values is thus determined by the mixing factor n, which can be obtained from the so-called "magic pentagon", displayed in Figure 4.1. The numbers in Figure 4.1 show the magnitude in which g_i shifts due to orbital mixing along axis i. The colors represent the direction of the overlap: green is in the x-direction, blue is in the y-direction and red is in the z-direction. In a molecule with a mirror plane in x-y and the SOMO is the d_{z^2} orbital, there is no orbital mixing possible in the z-direction, thus $g_z = g_e$. The g_z value in the case of the complex described in this chapter is also called $g_\perp$. Mixing in the x- and y-direction is equal resulting in only one g-value, which is called $g_\parallel$. In case the SOMO is the $d_{x^2-y^2}$, orbital mixing occurs in both xy and z direction. The orbital mixing in x- and y-direction has the same magnitude, resulting in one $g_\parallel$ value. The orbital mixing in z-direction is now larger than the mixing in the xy-plane. This results in a larger $g_\perp$ than $g_\parallel$ (Figure 4.1).

The values for $g_\perp$ and $g_\parallel$ were obtained by fitting the EPR spectra using Win95EPR. The geometry assignment was made on basis of the positions of $g_\perp$ and $g_\parallel$.

The structure of the *in situ* generated copper-phenanthroline complexes do not differ greatly

Table 4.1: *EPR parameters of in situ generated Cu(II) complexes with 1,10-phenanthroline ligands from 0.1 mM* Cu^{II} *and varying 1,10-phenanthroline concentrations in 0.1 M phosphate buffer, 0.05 M NaCl, acidified to pH 4 using HCl.*

[phen]	$g_\perp$	$g_\parallel$	*SOMO*	*Geometry*
0.1 mM	2.05	2.25	$d_{x^2-y^2}$	Elongated octahedron
0.2 mM	2.17	2.03	d_{z^2}	Trigonal bipyramid
0.3 mM	2.17	2.03	d_{z^2}	Trigonal bipyramid
0.4 mM	2.17	2.02	d_{z^2}	Trigonal bipyramid
0.5 mM	2.18	2.01	d_{z^2}	Trigonal bipyramid
0.6 mM	2.18	2.01	d_{z^2}	Trigonal bipyramid
0.7 mM	2.17	2.04	d_{z^2}	Trigonal bipyramid
0.8 mM	2.17	2.01	d_{z^2}	Trigonal bipyramid
0.9 mM	2.18	2.02	d_{z^2}	Trigonal bipyramid
1.0 mM	2.17	2.03	d_{z^2}	Trigonal bipyramid

if a 1,10-phenanthroline to copper ratio of 2:1 or higher is used (Figure 4.2 and Table 4.1). The $g_\parallel$ value is either 2.17 or 2.18 and the $g_\perp$ values range from 2.01 to 2.04. These values are slightly higher than the values found for copper-phenanthroline complexes in a previous study.[13] The values of 2.17 and ∼2.0 indicate a trigonal bipyramidal structure, with the SOMO being the d_{z^2} orbital. With a one to one ratio of copper to phenanthroline, the $g_\parallel$ value is 2.05, while the $g_\perp$ value is higher and found at 2.25. This is indicative of a complex with an elongated octahedron geometry with the SOMO being the $d_{x^2-y^2}$ orbital.

The structure of two similar *in situ* generated 10 to 1 complexes with 2-2'-bipyridine (bipy) and 4,7-dimethyl-1,10-phenanthroline (DMP) ligands were recorded by EPR as well. The g-values for 10 to 1 ligand to Cu^{II} complexes with both the DMP and bipy ligands are very similar to the 1,10-phenanthroline complex, indicating the copper complexes are also in the trigonal bipyramidal geometry.

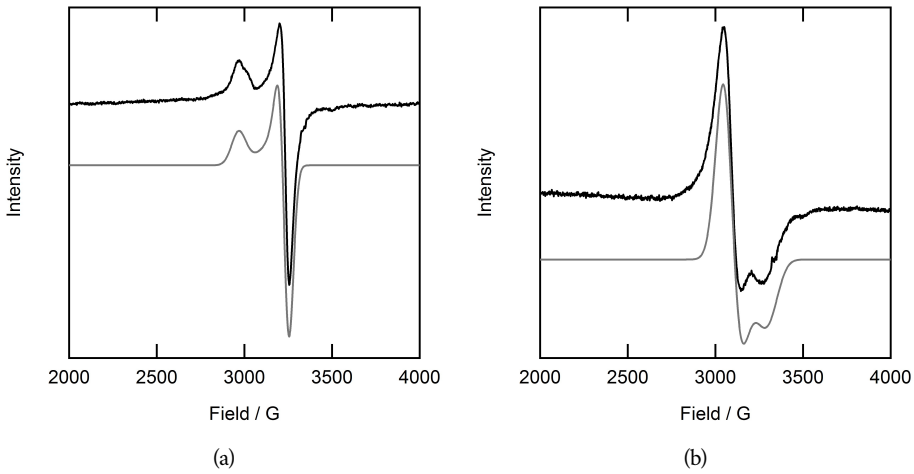

Figure 4.2: X-band EPR spectra (black lines) and simulations (grey lines) of solutions of 0.1 mM Cu^{II} with a) 0.1 mM and b) 0.2 mM phen in 0.1 M phosphate buffer and 0.05 M NaCl acidified to pH 4 using HCl at 78 K.

4.3.2 Electrochemistry of an *in situ* generated copper-phenanthroline complex

Copper-phenanthroline was formed *in situ* in solution by preparing an electrolyte solution with 1 mM Cu^{II} and 1 mM 1,10-phenanthroline and 1 mM Cu^{II} and 2 mM 1,10-phenanthroline in 0.1 M phosphate buffer containing 0.05 M NaCl acidified to pH 4 using HCl. No well-defined redox couples were observed in an electrolyte solution containing 1 mM Cu^{II} and 1 mM 1,10-phenanthroline (Figure 4.3). A reductive peak is observed at 0.45 V. In the positive going scan, an oxidative wave is observed from approximately 0.45 V up to the vertex potential of 0.75 V. In the cyclic voltammogram at a gold electrode in argon-purged electrolyte a well-defined redox couple at 0.41 V *versus* RHE was observed at a scanrate of 100 mV s^{-1}, together with two oxidation event around 0.6 and 0.7 V *versus* RHE (Figure 4.3). A single redox couple is observed if the upper vertex is kept below 0.11 V.

Due to the high ligand exchange rate of copper ions, a higher concentration of phenanthroline to copper is expected to yield more $[Cu^{II}(phen)_2L_x]^{+/2+}$ (where L is Cl^- or H_2O) and

Table 4.2: *EPR parameters of in situ generated Cu(II) complexes with different ligands from 0.1 mM Cu^{II} and 1 mM ligand in 0.1 M phosphate buffer, 0.05 M NaCl, acidified to pH 4 using HCl.*

Ligand	$g_\perp$	$g_{\|\|}$	*Ground state*	*Geometry*
phen	2.17	2.03	d_{z^2}	Trigonal bipyramid
bipy	2.17	2.01	d_{z^2}	Trigonal bipyramid
DMP	2.17	2.01	d_{z^2}	Trigonal bipyramid

thus more stable complex in solution. Even though EPR spectroscopy does not show any structural changes above a 1:2 ratio of Cu^{II} to 1,10-phenanthroline, the influence of the ratio was investigated using cyclic voltammetry as well.

Since the solubility of 1,10-phenanthroline in water is rather low (14.9 mM at 20 °C),[14] a lowering of the copper and phenanthroline concentrations compared to the cyclic voltammetry described above was needed to dissolve the phenanthroline in the electrolyte solution. The copper concentration was decreased tenfold to 0.1 mM. With an increasing 1,10-phenanthroline to copper ratio the Cu^{I}/Cu^{II}) redox couple became more reversible (Figure 4.4). Similarly to Figure 4.3 but at a 0.1 mM concentration of copper and 1,10-phenanthroline(thus at a 1:1 ratio of 1,10-phenanthroline to Cu^{II}) no reversible redox behavior is observed whatsoever. The $E_{1/2}$ shifts from 0.41 V at a 2:1 ratio to 0.34 V at a 10:1 ratio of 1,10-phenanthroline to Cu^{II}. This indicates that the balance shifts from free Cu^{2+} and $[Cu^{II}(phen)L_x]^{+/2+}$ to $[Cu^{II}(phen)_2L_x]^{+/2+}$ at a high concentration of 1,10-phenanthroline.

The redox behavior of complexes with bipy and DMP ligands was investigated in a 1 to 10 copper to ligand ratio. Cyclic voltammetry was performed with an *in situ* generated complex from 1 mM bipy and 0.1 mM Cu^{II} in 0.1 M phosphate buffer with 0.05 M NaCl acidified to pH 4 using HCl. In the cyclic voltammogram two redox events are observed (Figure 4.5a). A reversible redox couple is visible at 0.39 V *verus* RHE with low peak separation. A low peak separation is indicative of a surface adsorbed species. Between 0.6 and 0.7 V, an oxidative peak is observed, which is accompanied by a reductive peak at 0.52 V *versus* RHE. At high scanrate, the oxidative peak between 0.6 and 0.7 V broadens and the oxidative wave of the reversible redox couple at

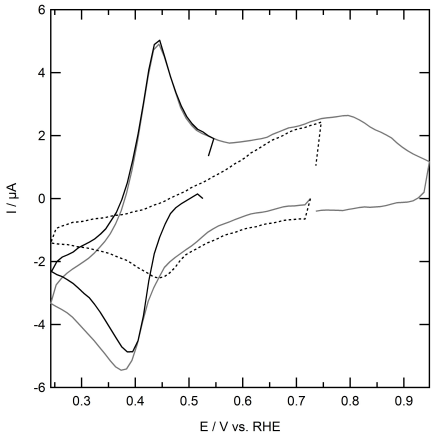

Figure 4.3: Cyclic voltammogram of a gold electrode under argon in a 1 mM solution of $Cu^{II}$and 2 mM 1,10-phenanthroline (solid lines) and in a 1 mM solution of $Cu^{II}$and 1 mM 1,10-phenanthroline (dotted line) in a 0.1 M phosphate buffer with 0.05 M NaCl acidified to pH 4 at 100 mV s^{-1}.

0.39 V is no longer visible.

In the cyclic voltammogram of *in situ* generated copper-DMP complexes from 1 mM DMP and 0.1 mM Cu^{II} in 0.1 M phosphate buffer with 0.05 M NaCl acidified to pH 4 using HCl irreversible behavior of the Cu^{I}/Cu^{II} redox couple is observed (Figure 4.5b). The separation of the peaks ranges between 470 mV at 10 mV s^{-1} to 660 mV at 500 mV s^{-1} and is thus very large. A large peak separation, and therefore irreversible redox behavior, suggests that copper deposits are being formed. It was therefore not further investigated.

By calculating the peak current of either the reduction or the oxidation process of a reversible redox process, the homogeneity of a molecular process can be determined. For one-electron transfer processes in solution, a linear relationship between the peak current and the squire root of the scanrate is expected, according to the Randles Cevčik relation (Equation 4.2), where i_p is the peak current, *n* is the number of electrons, *F* is the Faraday constant, ν is the scanrate, *A* is the electrode area D_0 is the diffusion constant, *R* is the gas constant and *T* is the temperature. For the Randles Cevčik relation, the peak position of the redox couple needs to be constant with

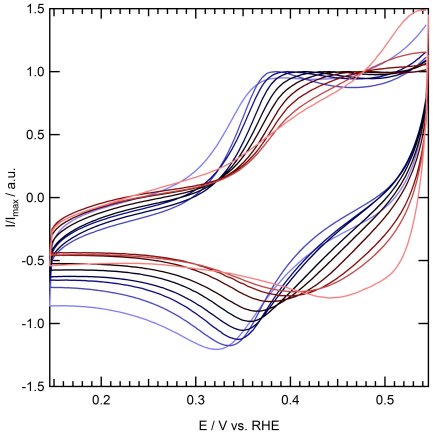

Figure 4.4: Cyclic voltammograms with a range of 1,10-phenanthroline concentration from 1 mM (blue line) to 0.1 mM (red line) and 0.1 mM of Cu^{II} in a 0.1 M phosphate buffer with 0.05 M NaCl acidified to pH 4 at 100 mV s^{-1}.

changing scanrate.

$$i_p = 0.466nFAC^0 \left(\frac{nF\nu D_0}{RT}\right)^{1/2} \tag{4.2}$$

The peak position of the redox couples of cyclic voltammograms of *in situ* generated complexes from 1 mM 1,10-phenanthroline and 0.1 mM Cu^{II} stays the same while changing the scanrate from 10 to 500 mV s^{-1} with $E_{1/2}$ = 0.81 V *verus* RHE (Figure 4.6). At scanrates of 200 mV s^{-1} and higher (blue lines), the oxidative peak becomes less well-defined. Therefore the reductive peak was used to investigate the homogeneity of the catalytic process.

The peak current of cyclic voltammograms with a 10:1 ratio of ligand to Cu^{II} is linear with the square root of the scanrate (Figure 4.7). Moreover, the trend line goes through the origin when it is extrapolated. This indicates the complex behaves as a dissolved molecular species which exhibits one-electron transfer to the working electrode. The complex in solution has the trigonal bipyramidal geometry with two 1,10-phenanthroline ligands attached to the copper ion, as was described in the EPR section *vide supra*.

The oxygen reduction reaction was investigated on a bare gold electrode and with *in situ*

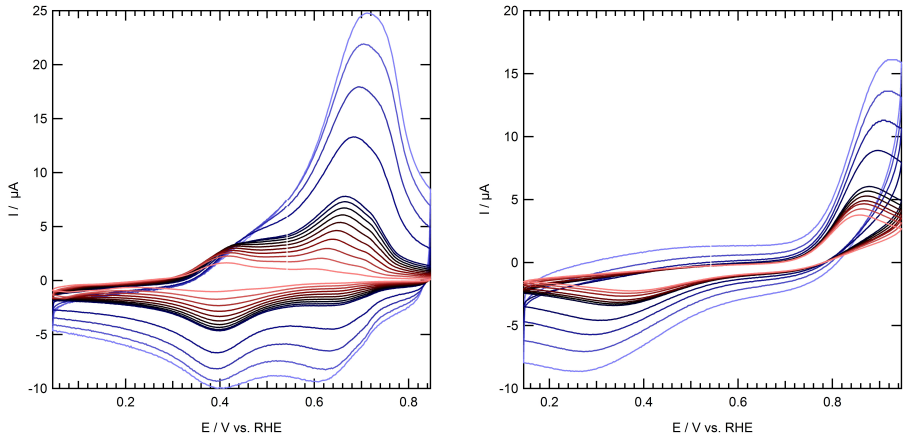

Figure 4.5: Cyclic voltammogram at scanrates from 10 (red line) to 500 (blue line) mV s^{-1} of a gold electrode with 1 mM solutions of a) 2,2'-bipyridine and b) 4,9-dimethyl-1,10-phenanthroline together with 0.1 mM Cu^{II}, 0.1 M phosphate buffer and 0.05 M NaCl acidified to pH 4 using HCl.

generated copper phenanthroline complexes (Figure 4.8). On a bare gold electrode, oxygen reduction starts at 0.36 V *versus* RHE. A maximum activity of -20 µA at the vertex potential of 0.24 V *versus* RHE is observed. Oxygen reduction with an *in situ* generated complex from 1 mM 1,10-phenanthroline and 0.1 mM Cu^{II}, a reductive current is observed starting around 0.44 V *versus* RHE. A starting potential of 0.44 V indicates a high overpotential of 800 mV. A shoulder is observed around 0.35 V, the same potential where oxygen reduction started on a bare gold electrode. The maximum activity of 11 µA is observed at the vertex potential of 0.24 V, which is lower than the activity on the bare gold electrode at the same potential. With oxygen reduction by *in situ* generated copper complex with 3 mM 1,10-phenanthroline and 1 mM Cu^{II}, an onset potential of 0.41 V *versus* RHE is observed, similar to the onset potential of the bare gold electrode. The maximum activity is 13 µA at the vertex potential of 0.24 V, which is slightly higher than the 10:1 complex, but still lower than the bare gold electrode. When the complexes from 1 mM Cu^{II} and 2 mM 1,10-phenanthroline are generated *in situ*, the onset potential is 0.44 V *ver-*

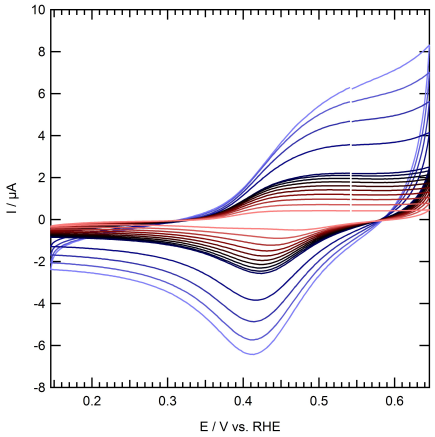

Figure 4.6: Cyclic voltammograms of a gold electrode under argon in a 1 mM solution of Cu^{II} and 2 mM 1,10-phenanthroline in a 0.1 M phosphate buffer with 0.05 M NaCl acidified to pH 4 at 500 (top blue line) to 10 mV s^{-1} (lowest orange line).

sus RHE, which is the same as the 0.1 mM Cu^{II} and 1 mM 1,10-phenanthroline situation. From 0.3 V, the current increases in line with the profile of the bare gold electrode, albeit the current is slightly lower than that of the bare gold. The maximum current is observed at the vertex potential and is 18 µA. The observed current for 1 mM 1,10-phenanthroline with 1 mM Cu^{II} in solution differs greatly from the other measurements. The current starts increasing at 0.45 V and keeps increasing until it reaches a plateau at 0.38 V *versus* RHE. The maximum current observed is 23 µA. The current observed is thus higher than the bare gold electrode and has a higher start potential than the gold electrode. The reductive current indicated the *in situ* generated complex is an active oxygen reduction catalyst.

4.4 Discussion

The fast ligand exchange kinetics of copper complexes in combination with the redox processes taking place in an electrochemical cell account for a complex picture regarding which species present in the electrolyte solution and which species is responsible for the oxygen reduction catalysis. As far as the ligand exchange equilibria are concerned, zero (free copper), one or two

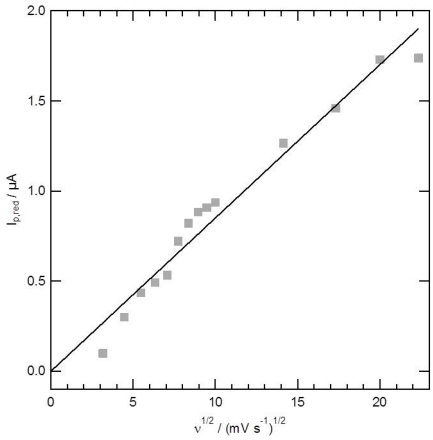

Figure 4.7: Peak current of the reduction peak *versus* the square root of the scanrate for the investigation of the homogeneity of the *in situ* generated copper-phenanthroline complex.

1,10-phenanthroline ligands can be ligated to copper. In the potential window where oxygen reduction is taking place, Cu^0, Cu^I and Cu^{II} can be expected. This leads to the following equilibria that need to be taken into account.

$$Cu^0 \rightleftharpoons Cu^I + e^- \tag{4.3}$$

$$Cu^0 \rightleftharpoons Cu^{II} + 2e^- \tag{4.4}$$

$$Cu^IL \rightleftharpoons Cu^{II}L + e^- \tag{4.5}$$

$$Cu^IL_2 \rightleftharpoons Cu^{II}L_2 + e^- \tag{4.6}$$

$$Cu^{II} + L \rightleftharpoons Cu^{II}L \tag{4.7}$$

$$Cu^I + L \rightleftharpoons Cu^IL \tag{4.8}$$

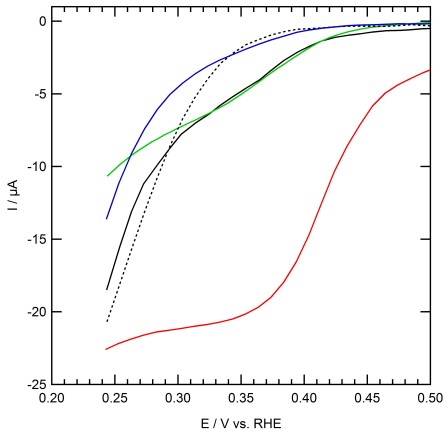

Figure 4.8: Oxygen reduction at a gold electrode with *in situ* generated copper-phenanthroline complexes with 0.1 mM Cu^{II} and 1 mM 1,10-phenanthroline (green line), 1 mM Cu^{II} and 1 mM 1,10-phenanthroline (red line), 1 mM Cu^{II} and 2 mM 1,10-phenanthroline (black solid line), 1 mM Cu^{II} and 3 mM 1,10-phenanthroline (blue line) and without any catalyst in solution (black dotted line) in a 0.1 M phosphate buffer with 0.05 M NaCl acidified to pH 4 using HCl.

$$Cu^{II}L + L \rightleftharpoons Cu^{II}L_2 \tag{4.9}$$

$$Cu^{I}L + L \rightleftharpoons Cu^{I}L_2 \tag{4.10}$$

Equations 4.3 and 4.4 is the deposition of free copper from solution onto the electrode. The reactions can happen coupled to Equations 4.7 and 4.8, which are the dissociation of the only 1,10-phenanthroline ligand on the copper center. Upon dissociation of the ligand, free copper is formed which can deposit electrochemically to the electrode surface. The deposit formed on the electrode is apparently not active in the oxygen reduction reaction. Equations 4.5 and 4.6 display the redox couple of the Cu^{I}/Cu^{II} complexes in solution. Equation 4.5 is the irreversible redox couple observed in the 1:1 ligand to copper ratio, while Equation 4.6 is the reversible redox couple observed when a ratio of 2:1 and higher is used. Based on the oxygen reduction activity displayed in Figure 4.8 the (reduced form of) $Cu^{II}L_2$ is inactive towards oxygen reduction as the activity observed is similar to that of a bare gold electrode. The catalytically active species is most likely the reduced form of $Cu^{II}L$ complex, which is predominantly present when a 1:1 ratio of copper ions to 1,10-phenanthroline is used (Figures 4.2 and 4.8).

The adsorbed $[Cu^{II}(DMP)]^{2+}_{ads}$ complex reported by Anson and Zhang has a 280 mV lower overpotential than the 1:1 copper to 1,10-phenanthroline complex in this paper.[10] A comparison of the electrochemical activity is difficult as there is no electrode surface area reported in the report by Anson and Zhang. The oxygen reduction reaction with *in situ* generated complexes

$[Cu(tmpa)(CH_3CN)](OTf)_2$ (tmpa = tris(2-pyridylmethyl)amine) is a catalyst for the electroreduction of oxygen developed in our group.[15] Both the complex $[Cu(tmpa)(CH_3CN)](OTf)_2$ and the *in situ* generated complex with a 1:1 ratio ligand to copper have one ligand attached to the copper. However the tmpa ligand has 4 coordinating nitrogen atoms which compares to two in 1,10-phenanthroline. Given that the copper center in the complex $[Cu(tmpa)(CH_3CN)](OTf)_2$ is ligated by four nitrogen donors, it is remarkable that the 2:1 complex of 1,10-phenanthroline to copper shows no activity towards oxygen reduction whatsoever.

The catalytic activity of the $[Cu(tmpa)(CH_3CN)](OTf)_2$ system is thereby significantly faster than the 1:1 complex of 1 mM Cu^{II} and 1,10-phenanthroline investigated in this work. A catalytic oxygen reduction current of approximately 1.5 mA cm^{-2} is observed on glassy carbon

with 1.0 μM [Cu(tmpa)(CH_3CN)]$(OTf)_2$ in solution whereas the Cu-phen complex obtains only 0.4 mA cm^{-2} at a 1 mM catalyst concentration. It would be interesting to compare the turnover frequencies of [Cu(tmpa)(CH_3CN)]$(OTf)_2$ and the 1:1 copper to 1,10-phenanthroline complex. Yet due to the irreversible behavior of the reduction of the this species, accompanied by deposition on the electrode obstructs us from using the foot of the wave analysis as performed in the [Cu(tmpa)(CH_3CN)]$(OTf)_2$ study.[15, 16] Since there is competition between oxygen reduction with a 1:1 copper complex and the formation of a copper deposit on the electrode surface, a strategy to prevent the formation of a copper deposit was developed. This is discussed in Chapter 5.

4.5 Conclusion

An active oxygen reduction catalyst is formed at a 1:1 phenanthroline to copper ratio. This complex does not show a reversible Cu^{I}/Cu^{II} redox couple. Therefore it is likely that formation of metallic copper on the electrode surface. We anticipate that immobilization of the gold surface with phenanthroline 1) prevents deposition of copper on gold even though free copper is present in solution and 2) spontaneously forms an active layer of copper phenanthroline species in the presence of copper salts in solution. This strategy is discussed in Chapter 5.

4.6 References

(1) Fernández, E. M.; Moses, P. G.; Toftelund, A.; Hansen, H. A.; Martínez, J. I.; Abild-Pedersen, F.; Kleis, J.; Hinnemann, B.; Rossmeisl, J.; Bligaard, T.; Nørskov, J. K. *Angew. Chem. Int. Ed.* **2008**, *47*, 4683–4686.

(2) Koper, M. T. M. *J. Electroanal. Chem.* **2011**, *660*, 254–260.

(3) Cracknell, J. A.; Vincent, K. A.; Armstrong, F. A. *Chem. Rev.* **2008**, *108*, 2439–2461.

(4) Reedijk, J. *Platin. Met. Rev.* **2008**, *52*, 2–11.

(5) Taube, H. *Chem. Rev.* **1952**, *50*, 69–126.

(6) Aznar, E.; Ferrer, S.; Borrás, J.; Lloret, F.; Liu-González, M.; Rodríguez-Prieto, H.; García-Granda, S. *Eur. J. Inorg. Chem.* **2006**, *2006*, 5115–5125.

(7) Thorum, M. S.; Yadav, J.; Gewirth, A. A. *Angew. Chem. Int. Ed.* **2009**, *48*, 165–167.

(8) Hoang, T. T. H.; Ma, S.; Gold, J. I.; Kenis, P. J. A.; Gewirth, A. A. *ACS Catal.* **2017**, *7*, 3313–3321.

(9) Van Dijk, B.; Hofmann, J. P.; Hetterscheid, D. G. H. *Phys. Chem. Chem. Phys.* **2018**, *20*, 19625–19634.

(10) Zhang, J.; Anson, F. C. *Electrochim. Acta* **1993**, *38*, 2423–2429.

(11) Zhang, J.; Anson, F. C. *J. Electroanal. Chem.* **1992**, *341*, 323–341.

(12) Lei, Y.; Anson, F. C. *Inorg. Chem.* **1994**, *33*, 5003–5009.

(13) Garribba, E.; Micera, G. *J. Chem. Educ.* **2006**, *83*, 1229.

(14) Burgess, J.; Haines, R. I. *J. Chem. Eng. Data* **1978**, *23*, DOI: 10.0.

(15) Langerman, M. P.; Hetterscheid, D. G. H. *Submitted*.

(16) Costentin, C.; Drouet, S.; Robert, M.; Savéant, J.-M. *J. Am. Chem. Soc.* **2012**, *134*, 11235–11242.